RSC Advances

ROYAL SOCIETY OF CHEMISTRY

www.rsc.org/advances

RSC Advances

RSCPublishing

ARTICLE

Original biobased nonisocyanate polyurethanes: Solvent- and catalyst-free synthesis, thermal properties and rheological behaviour†

Camille Carré,[a] Lara Bonnet[a] and Luc Avérous*[a]

Thanks toCite this: DOI: 10.1039/x0xx00000x

Received 00th January 2012,
Accepted 00th January 2012

DOI: 10.1039/x0xx00000x

www.rsc.org/

Novel biobased NonIsocyanate PolyUrethanes (NIPU) were synthesized from dimer-based diamines and sebacic biscyclocarbonate in bulk, and without catalyst. All synthesized NIPU present biobased contents around 80 %. Biscyclocarbonates and final NIPU were characterized by FTIR and NMR spectroscopy. A specific study was conducted to determine the best carbonate to amine ratio. The influence on the structures and properties of NIPU with different average amine functionalities, varying from 2.0 to 2.2, was investigated by DSC, SEC and dynamic rheological analyses. Based on FTIR analyses, it was found that the stoichiometric ratio is optimal for the NIPU synthesis to obtain the highest molar masses with appropriate kinetics. However, results show that the molar masses (up to 22,000 g.mol^{-1}) were lower than conventional polyurethanes. A specific structuration due to a higher crosslink degree was observed when the average functionality of the dimer diamine increased. As expected, the glass transition temperature raises in this case. Crosslinked samples were synthesized with an average amine functionality of 2.15 and 2.2. A promising elastomer sample with elongation higher than 600 % was then obtained.

Introduction

Polyurethanes (PU) are traditionally synthesized from the reaction between polyols and isocyanates.[1] The latter are nevertheless dangerous for the human health. Some studies[2, 3] have clearly shown that isocyanates are harmful and potentially carcinogenic compounds. A repetitive exposure to them can lead to serious and incurable respiratory problems.[4] Moreover, the synthesis of isocyanates requires the use of noxious substances such as phosgene. These different issues can find a global answer with a new range of biobased NonIsocyanate PolyUrethanes (NIPU), since a significant and growing attention is nowadays paid to environmental and health concerns.

Various synthetic strategies to obtain isocyanate- and phosgene-free PU were reported the last few years.[5-8] The three most studied reactions are AB-type azide condensation,[9] transurethane polycondensation,[8, 10] and aminolysis.[11-13] PU can indeed be prepared without isocyanate, *via* the amine-cyclocarbonate aminolysis reaction. Cyclic carbonates react with amines to form urethane, or more specifically hydroxyurethane bonds. According to the ring opening step, primary or secondary hydroxyl groups can be obtained. However, in the case of polymerization, mainly hybrid PU having both primary and secondary alcohols are formed[14, 15] These NIPU are also called polyhydroxyurethanes (PHU).

In the literature, the synthesis of NIPU led to two major issues: (i) final low molar masses and (ii) slow kinetics, which are serious impediments to their developments. To overcome some of these drawbacks, some studies were carried out with various catalysts to enhance the reactivity of the reaction.[16, 17] In particular, the use of lithium chloride and triazabicyclodecene seems to be promising, but at the moment their efficiencies are too limited. An answer to obtain materials with high properties, and economically viable, is to use crosslinked systems to obtain high molar masses. Two strategies can be adopted. The first way is to employ polyfunctional cyclic carbonates obtained from raw triglycerides of soybean or linseed oil *via* an epoxydation/carbonatation route.[18, 19] The second path is to use polyfunctional amines as curing agents, such as tris(2-aminoethyl)amine, polyethylenimine or citric acid aminoamides.[20] With such polyfunctional reagents, crosslink is then possible. Recently, Figovsky *et al.* have developed a hybrid NIPU-like coating marketed under the name Green Polyurethane^{TM}, which is based on cyclocarbonates and amines with epoxy functions.[21-23]

Cyclic carbonates can be synthesized by various methods[24] such as the direct esterification of carboxylic acids with glycerol carbonate. The latter appears to be a promising route in the frame of a new emerging challenge based on the use of renewable resources. Glycerol carbonate, a cheap and widely available biobased building block, can result from the reaction between carbon dioxide and glycerol, a major by-product from

e.g., the biodiesel industry.[25] Carboxylic acids can also be produced from biobased feedstocks and more particularly from vegetable oils. For instance, sebacic acid is industrially obtained at low cost by alkali fusion (heating with soda under oxidative conditions) at 250-280 °C, from ricinoleic acid extracted from castor oil.[26] Sebacic acid is often chosen as a chemical for synthesis, since it is a biobased diacid with a 10-carbon chain length, and largely and commercially available. Then, it could be a good candidate for the synthesis of bicyclocarbonates by esterification.

Several syntheses between biscyclocarbonates and various diamines were described in the literature and the relationships between structure and reactivity were analysed to a large extent.[27-29] Tomita *et al.* carried out studies on the reactivity of different cyclocarbonates.[28, 29] They showed that the nature of the substituent on the cyclic carbonate and the number of atoms involved on the cyclocarbonate ring have an impact on their reactivity towards diamines.

Various diamines have already been reported for NIPU synthesis. According to Diakoumakos *et al.*, the structure and the molar mass of the diamines influence their reactivity with cyclocarbonates.[27] The authors demonstrated that low molar mass aliphatic amines present the highest reactivity. However, it was also proved that secondary amines can react with cyclic carbonates.[30] As far as we know, dimer fatty amines have never been reported for NIPU synthesis and present inherent specific characteristics. Compared with conventional diamines, they are biobased building blocks with 100 % renewable carbon content. Due to their structure with pending chains, the dimer diamines bring a high flexibility and a low glass transition temperature suitable for the elaboration of elastomeric polymers. Besides, the dimer diamines show a low viscosity, which is required for solvent-free synthesis. Moreover, they are commercially available. The dimer diamines are derivatives of fatty acids obtained from a dimerization process (Diels Alder reaction). As their corresponding dimer fatty acids, they can be used as building blocks for the elaboration of several biobased macromolecular architectures.[31, 32] An example of corresponding chemical structure is given by Fig. 1.

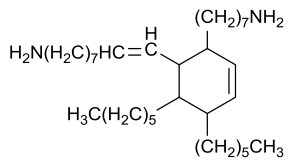

Fig. 1 Dimer diamine molecular structure.

In the present study, we have chosen to elaborate new biobased NIPU *via* a green chemical pathway *i.e.*, without solvent and catalyst systems.

The aim of this study is to synthesize biobased NIPU by bulk polymerization between sebacic biscyclocarbonate (SB BisCC) and dimer-based diamine (DDA), as illustrated in Fig. 2, and to analyse their corresponding structure-properties relationships. In that frame, the effects of five different average amine functionalities, from 2.0 to 2.2, referred to as *NIPU-fn=2.0, 2.05, 2.1, 2.15* and *2.2* respectively, were considered to modulate the crosslink degree of the samples. The chemical characterization of the NIPU systems, the effect of the carbonate:amine ratio and their corresponding physical and thermal properties were investigated. The rheological behaviour of the corresponding products was also studied. Additional experiments based on specific *NIPU-fn=2.15* and *2.2* were carried out to provide a better characterization and understanding of these promising biobased crosslinked materials.

Experimental

Materials and chemicals

Sebacoyl chloride (97 %) was purchased from Alfa Aesar (Karlsruhe, Germany). Glycerol carbonate (Jeffsol GC, 93 %) was obtained from Huntsman (Everberg, Belgium). Dimer diamines (DDA) commercially available under the trade name Priamine were kindly supplied by CRODA (Goole, England). DDA are C36-biobased molecules obtained from the dimer fatty acid (Fig. 1). Two grades of DDA, hereinafter referred to as DDA1 and DDA2, were used alone or mixed together to adjust a precise average amine functionality. DDA1 has an average functionality of 2.2 (dimer content = 75 %) and DDA2 of 2.0 (dimer content > 99 %), respectively. They present an amine value (AV) of 198 and 204 mg KOH/g, respectively, with glass transition temperatures lower than -50 °C. At room temperature, DDA1 is an amber, viscous liquid and DDA2 is a yellowish, slightly viscous liquid. All chemicals were used as received without any purification.

Syntheses

Synthesis of sebacic biscyclocarbonate (SB BisCC). The sebacic biscyclocarbonate was synthesized following the pathway given by Fig. 2. The glycerol carbonate (20 g, 170 mmol) was mixed with freshly distilled dichloromethane (60 mL) and triethylamine (8.6 g, 85 mmol) under a light stream of inert gas. The flask was cooled in an ice water bath. Sebacoyl chloride (18.5 g, 77.3 mmol) was added dropwise to the stirred reaction mixture.

RSC Advances

RSCPublishing

ARTICLE

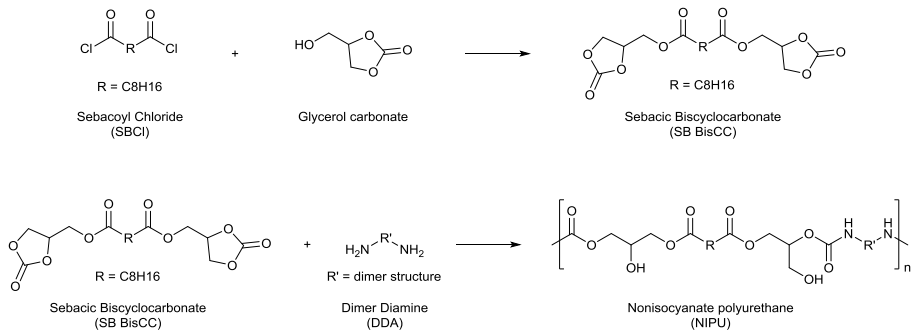

Fig. 2 Esterification of sebacoyl chloride to yield sebacic biscyclocarbonate (SB BisCC) followed by aminolysis of SB BisCC with dimer-based diamine.

After an overnight reaction, triethylamine hydrochloride NEt_3•HCl was taken out by filtration, and the phase was washed with a 5 wt% HCl solution and water, to eliminate the excess of glycerol carbonate. The solution was then dried with anhydrous sodium sulphate. Solvent was removed under vacuum to yield 22-23 g (71-77 %) of white powder.

The structure of SB BisCC was determined and confirmed by ^{1}H- (Fig. 3) and ^{13}C-NMR spectra (see Fig. S1 in the ESI†). On the FTIR spectrum, the characteristic peaks of the ester and cyclocarbonate functions were 1740 cm^{-1} and 1796 cm^{-1}, respectively (see Fig. S2 in the ESI†).

^{1}H-NMR (400 MHz, $CDCl_3$, δ, ppm): 1.32 (8H, s, -OCO-C*H*$_2$-CH$_2$-CH$_2$-), 1.64 (4H, t, J = 7.1 Hz, -OCO-CH$_2$-C*H*$_2$-CH$_2$-), 2.38 (4H, t, J = 7.5 Hz, -OCO-C*H*$_2$-CH$_2$-CH$_2$-), 4.15; 4.55 (8H, m; t, J = 8.6 Hz, -OCO-C*H*$_2$-CH-C*H*$_2$-O-) and 4.9 (2H, m, -OCO-CH$_2$-C*H*-CH$_2$-O-);

^{13}C-NMR (100 MHz, $CDCl_3$, δ, ppm): 24.7 (-OCO-CH$_2$-*C*H$_2$-CH$_2$-), 28.9 (-OCO-CH$_2$-CH$_2$-*C*H$_2$-), 33.8 (-OCO-*C*H$_2$-CH$_2$-CH$_2$-), 62.8 (-OCO-CH$_2$-CH-*C*H$_2$-O-), 66.0 (-OCO-*C*H$_2$-CH-CH$_2$-O-), 73.8 (-OCO-CH$_2$-*C*H-CH$_2$-O-), 154.4 (-OCOO- from the cyclocarbonate ring) and 173.2 (-O*C*O-CH$_2$-CH$_2$-CH$_2$-);

FTIR-ATR (cm^{-1}): 1740 (-COO-) and 1796 (-OCOO-).

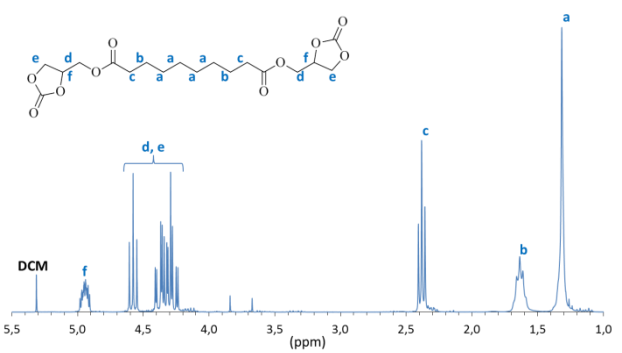

Fig. 3 ^{1}H-NMR of SB BisCC.

Synthesis of NIPU. In a 100 mL reactor equipped with a mechanical stirrer, sebacic biscyclocarbonate (20 g, 49.7 mmol) and diamine, or a mix of both diamines, were added at a molar stoichiometric ratio, according to the second chemical equation given by Fig. 2. The reaction took place in bulk without catalyst, at a temperature of 75 °C, and under inert gas flow to avoid the amine carbonatation during the synthesis. After two hours under stirring, the viscous mixture was spread on a plate covered with a Teflon® sheet and heated in an oven under vacuum at 75 °C for ninety-four hours. The product was obtained as a yellow or brown solid depending on the DDA used.

^{1}H-NMR (400 MHz, $CDCl_3$, δ, ppm, Fig. 4): 0.88 (6H$_m$ from DDA dangling chains, s, -CH$_3$), 1.20-1.40 (4H$_f$ and H$_c$ from DDA structure, m, -CH$_2$-), 1.50 (4H$_b$, s, -CH$_2$-), 1.63 (4H$_e$, s, -CH$_2$-), 2.36 (4H$_d$, t, J = 7.41 Hz, -CH$_2$-), 3.18 (4H$_a$, m, -CH$_2$-), 3.63 (0.6H$_g$, m, -CH$_2$-), 3.72 (0.6H$_i$, m, -CH$_2$-), 4.07 (0.7H$_k$, m, -CH=), 4.10-4.36 (2.8H$_{j,l,\ m}$, -CH$_2$-) and 5.00 (0.3H$_h$, m, -CH=);

^{13}C-NMR (100 MHz, $CDCl_3$, δ, ppm, see Fig. S3 in the ESI†): 14.2 (-CH$_3$), 22.7 and 28.9-32.0 (-OCO-CH$_2$-CH$_2$-*C*H$_2$- and -*C*H$_2$ from DDA structure), 24.8 (-OCO-CH$_2$-*C*H$_2$-CH$_2$-), 26.8 (-OCO-NH-CH$_2$-*C*H$_2$), 33.8 (-OCO-*C*H$_2$-CH$_2$-CH$_2$-), 41.3 (-OCO-NH-*C*H$_2$-CH$_2$-R-), 62.5 (-COO-CH$_2$-CH-*C*H$_2$-OH), 63.2 (-COO-*C*H$_2$-CH-CH$_2$-OH), 65.1 (-NH-COO-*C*H$_2$-CHOH-CH$_2$-), 66.0 (-NH-COO-CH$_2$-CHOH-*C*H$_2$-), 68.6 (-NH-COO-CH$_2$-*C*HOH-CH$_2$-), 70.7 (-COO-CH$_2$-*C*H-CH$_2$-OH), 156.8 (O*C*ONH) and 174.0 (-O*C*O-CH$_2$-CH$_2$-CH$_2$-);

FTIR-ATR (cm^{-1}, see Fig. S4 in the ESI†): 1247 (=CO stretching, s), 1536 (-NH bending, m), 1701 (-C=O stretching of urethane and ester, s, broad) and 3335 (-NH and –OH stretching, respectively m and s, broad).

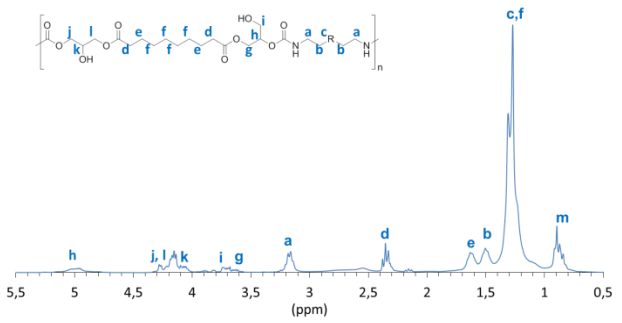

Fig. 4 ^{1}H-NMR of *NIPU-fn=2.0*.

General characterization techniques

Infrared spectroscopy was achieved with a Fourier transformed infrared spectrometer Nicolet 380 (Thermo Electron Corporation) working in Reflection Mode and equipped with an ATR diamond module (FTIR-ATR). The FTIR-ATR spectra were collected at a resolution of 4 cm^{-1} and with 64 scans per run.

^{1}H- and ^{13}C-NMR spectra were recorded on a Bruker Ascend^{TM} 400 spectrometer at 400 MHz and 100 MHz respectively. Chloroform-d_6 was used as a solvent.

Thermal degradation was studied by thermogravimetric analyses (TGA). Measurements were conducted under dry nitrogen (flow rate = 25 $mL.min^{-1}$) using a Hi-Res TGA Q5000 apparatus from TA Instruments. The samples (3–5 mg placed in an aluminium pan) were heated up to 650 °C at 10 $°C.min^{-1}$. The characteristic degradation temperatures are the temperatures at the maxima of the derivative thermogram (DTG) curves (T_{max}).

The main characteristic temperatures were determined by differential scanning calorimetry (DSC Q200, TA Instruments) under nitrogen flow. The samples (2–5 mg) were heated until 175 °C with a heating rate of 10 $°C.min^{-1}$ (first heating scan), then cooled to −80 °C at 5 $°C.min^{-1}$ and finally re-heated to 175 °C at a heating rate of 10 $°C.min^{-1}$ (second heating scan). The glass transition temperatures (T_g) was determined as midpoints of the change in slop of the baseline. These values were obtained from the second heating scan in order to erase the previous thermal history of the samples during the first scan.

The number average molar mass (M_n), the weight average molar mass (M_w) and the dispersity (Đ) of the resulting samples were determined by Size Exclusion Chromatography (SEC), using a Malvern Instrument apparatus (Viscotek RImax). This device was equipped with a guard column 10 mm (8 µm) and three 300 mm columns (50, 150 and 500 Å). Refractive index (RI) and ultra-violet (UV) detectors were used. Tetrahydrofuran (THF) was used as the eluent at a flow rate of 1 $mL.min^{-1}$. The apparatus was calibrated with linear polystyrene standard from 162 to 20,000 $g.mol^{-1}$.

Dynamic rheological analyses (DRA) of final materials were performed by using a strain-controlled rheometer (ARES, Rheometric Scientific) equipped with parallel-plate geometries. The oscillatory measurements were carried out on 8 and 25 mm diameter plates, with 2 mm thickness. The following tests were conducted: (i) dynamic strain sweep to estimate the viscoelastic region of the samples, (ii) isofrequency dynamic temperature sweep test from 0 up to 160 °C at a frequency of 1Hz. Changes in the viscous and elastic, or storage, modulus (G'' and G', respectively) were registered, and the corresponding tan δ = G''/G' were determined.

Dynamic mechanical thermal analyses (DMTA) were performed on polymers (samples with dimensions around 23x4x1 mm) with RSA-II apparatus from TA Instruments equipped with a liquid-nitrogen cooling system. Experiments were recorded on films with traction mode at a maximum strain from 0.03 to 2 % and a frequency of 1 Hz. The samples were heated from -50 to 200 °C at a heating rate of 2 $°C.min^{-1}$.

Uniaxial tensile tests were achieved using an Instron machine (type 5567, serie H1592). The experiments were performed at room temperature, using a crosshead speed of 100 $mm.min^{-1}$ and a load cell of 5 kN sensitivity. After adjusting the parameters, experiments were carried out at least 3 times for each sample. Young's modulus (E), tensile strength at break (σ_{max}) and elongation at break (ε_{max}) were determined.

Results and discussion

NIPU synthesis and chemical characterisations

A first study based on the analysis of the SB BisCC:DDA ratio was conducted to determine the optimal ratio, for the NIPU synthesis. FTIR spectroscopy was used to highlight specific changes in hydroxyl and carbonyl vibrations which provide direct evidence of reactions between cyclocarbonate and amine reagents. FTIR spectra of NIPU show distinctive absorption bands of the urethane group at 3300-3400 cm^{-1}, 1700 cm^{-1} (merged with the ester absorption peak), 1535 cm^{-1} and 1245 cm^{-1}, respectively (Fig. 5). The absorption band at 3300-3400 cm^{-1} is also assigned to the hydroxyl group resulting from the carbonate opening. Hydroxyl and urethane groups are shown for all samples, which confirm the expected structure of NIPU, also known as polyhydroxyurethanes (PHU). The peak at 1790 cm^{-1} is assigned to the unreacted SB BisCC carbonyl and the absorption peak of the amide group resulting from the aminolysis of ester groups appears at 1650 cm^{-1}. The samples prepared with a carbonate:amine ratio of 1.1:1 present a significant amount of unreacted SB BisCC. The amide peak is hardly noticeable, indicating that the ester group aminolysis is not significant. Samples formed at a stoichiometric ratio display neither BisCC nor distinct amide absorption peaks, suggesting that the carbonate conversion to urethane is quite complete. Only few secondary reactions could occur. At a ratio 1:1.1, the amide absorption peak becomes stronger, highlighting the aminolysis of the ester groups. These results show the importance of a stoichiometric ratio to achieve a complete reaction and minimize the secondary reaction of ester aminolysis, which induces chains cleavage, according to the reaction given by Fig. 6. This result is in good agreement with previous observations from Javni *et al.*[18, 33]

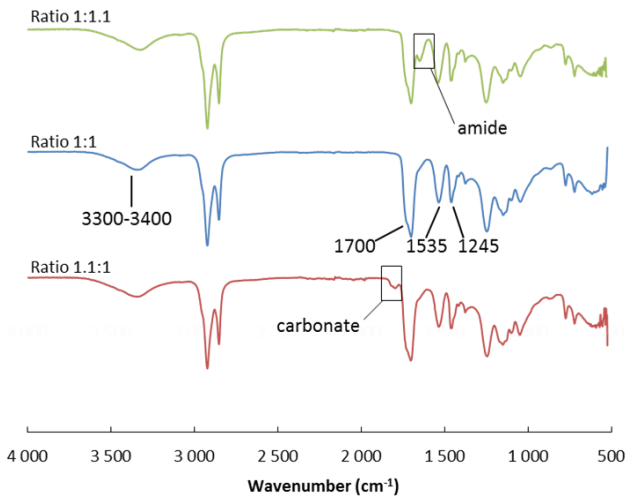

Fig. 5 FTIR spectra of *NIPU-fn=2.0* at different carbonate:amine ratios.

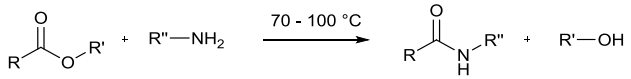

Fig. 6 Aminolysis of ester as side-reaction.

The number average molar masses (M_n) and the dispersity (Đ) of NIPU samples are summarized in Table 1, except for *NIPU-fn=2.15* and *2.2*, which were not soluble in THF.

Table 1 SEC results of NIPU samples.

NIPU sample	M_n (g.mol^{-1})	M_w (g.mol^{-1})	Đ
NIPU-fn=2.0	6,000	20,000	3.1
NIPU-fn=2.05	9,000	22,000	2.4
NIPU-fn=2.1*	7,000	18,000	2.5
NIPU-fn=2.15	*Not soluble in common solvents*		
NIPU-fn=2.2	*Not soluble in common solvents*		

* *Partially soluble.*

Compared with conventional PU obtained *via* the classic isocyanate-alcohol route,[34, 35] the molar masses and Đ obtained for the NIPU samples are quite lower and higher, respectively. This is due to the limited reactivity of the cyclocarbonate towards diamines, the existence of secondary reactions, such as the ester aminolysis, as well as the dimer diamine, which also presents a high Đ. However, molar masses are comparable to other NIPU systems[7, 36] and high Đ is also observed in PU formed with polyisocyanates and dimer derivatives.[32] A significant decrease of the molar mass is observed for *NIPU-fn=2.1*. Owing to an average amine functionality above 2.0, a part of the sample is crosslinked and thus not soluble. Consequently, only the soluble fraction with the lowest masses is analysed.

NIPU thermal properties

The thermal properties of NIPU were investigated by TGA and DSC to better understand the structure and the behaviour of the NIPU. The corresponding results are summarized in Tables 2 and 3, respectively.

TGA was used to investigate the influence of the average amine functionality on the thermal stability of the resulting synthesized polymers. Conventional PU are known to have a relatively low thermal stability, mainly because of the urethane bond reversibility.[37] In their study, Saunders *et al.* present a three-stage degradation mechanism of the urethane bond.[38] The first degradation step consists in the dissociation to isocyanate and alcohol. Then, the formation of primary amine and olefin occurs. Finally the third degradation step is the formation of secondary amine. As demonstrated by Javni *et al.*, these three reactions may proceed simultaneously.[39] TG curves (Fig. 7) indicated that thermal decomposition of NIPU started at 200 °C, after a slight mass decrease between 0 and 150 °C due to the vaporization of residual and linked water molecules. The thermal stability of these NIPU is similar to other NIPU from the literature,[40, 41] but lower than those of conventional dimer-based PU, which decompose above 300 °C.[42, 43]

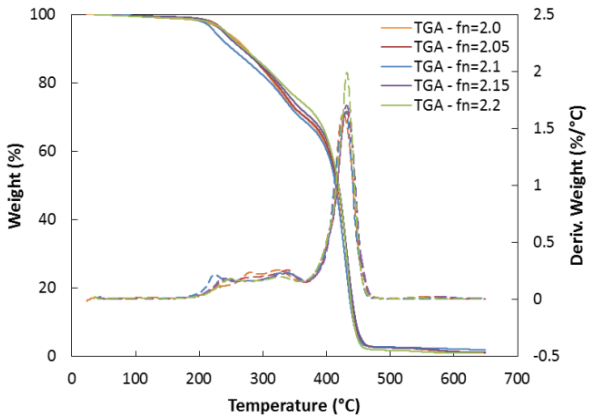

Fig. 7 TGA (solid line) and DTGA (dotted line) curves of NIPU under nitrogen.

It can be observed that the different NIPU materials show quite similar three-step degradation behaviours (Table 2). This result is not surprising considering that the PU structures are based on equivalent biscyclocarbonate and diamine building blocks. The two first degradation stages could be attributed to the degradation of the urethane linkages such as the ester bonds[44], which follows an irreversible mechanism starting from around 200 °C. The last degradation, which is more notable, could be attributed to the decomposition of the carbonated chains. For all samples, no difference between oxidative and inert atmosphere was noticed. Oxidation has no impact on thermal degradation.

Table 2 Main degradation temperatures for the different NIPU samples.

Samples	1st degradation stage		2nd degradation stage		3rd degradation stage	
	%deg	T_{max} (°C)	%deg	T_{max} (°C)	%deg	T_{max} (°C)
NIPU-fn=2.0	15	279	15	326	70	426
NIPU-fn=2.05	8	235	22	339	69	432
NIPU-fn=2.1	11	223	20	334	67	430
NIPU-fn=2.15	10	236	19	336	70	432
NIPU-fn=2.2	11	249	14	327	74	432

In the temperature domain explored by DSC, NIPU are not degraded (Table 2). Furthermore, neither endothermic nor exothermic phenomena were observed, indicating that all NIPU samples are fully amorphous. Their glass transition temperatures, T_g, are around -20 °C, between -23 and -14 °C (Table 3). DDA shows a hydrocarbonated cycle with pendant aliphatic chains, which raise free volume and then increase the

chains mobility. Such a particular structure is thus responsible of the low T_g observed for all NIPU samples. Equivalent T_g values are classically obtained for PU based on polyisocyanate or NIPU with dimer structures or pendant aliphatic fatty acid chains.[32, 36] Furthermore, we can notice that the T_g increases with the average functionality of the amine and thus with the crosslink degree of the polymers. The *NIPU-fn=2.15* and more especially the *NIPU-fn=2.2* samples differentiate from the others since their respective T_g are higher. Nevertheless, this trend is attenuated by two opposite behaviours. On the one hand, when increasing the average amine functionality, DDA masses should be enhanced to maintain a stoichiometric ratio. This means that when increasing the average amine functionality, the global T_g decreases. On the other hand, it is well known that the denser is the formed network, the less mobile are the polymer chains and thus the higher is the T_g. These last results show the effect of the monomer functionality on the final macromolecular architecture.

Table 3 Thermal properties of NIPU samples.

Samples	T_g (°C)
NIPU-fn=2.0	-23
NIPU-fn=2.05	-21
NIPU-fn=2.1	-22
NIPU-fn=2.15	-19
NIPU-fn=2.2	-14

Rheological behaviour of NIPU materials

To obtain additional and complementary information about the architectures and organisations of the NIPU, rheological analyses were carried out. Fig. 8 and 9 show the results of the dynamic rheological analyses of NIPU samples.

We can notice that the behaviour of the NIPU varies according to the amine functionality (Fig. 8). Between 80 and 120 °C, a rubbery plateau is observed for the NIPU samples with amine functionalities superior or equal to 2.15. This plateau shows a particular structuration of the polymer due to crosslinking points. In these cases, thermosets were obtained. Furthermore, the rubbery plateau of *NIPU-fn=2.2* is higher and longer than the one of *NIPU-fn=2.15* which indicates that the crosslink density is higher. The storage modulus of *NIPU-fn=2.2* is approximately equal to 10^4 Pa at 100 °C, which is lower than conventional thermosets whose moduli stay constant at about 10^6 Pa.[45] Below an average amine functionality of 2.2, the storage modulus (G') drops when increasing the temperature. The materials flow and thus are poorly or not structured. This phenomenon is highlighted at low average amine functionalities.

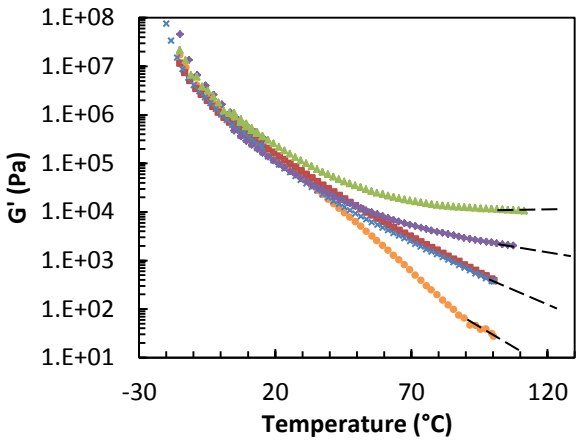

Fig. 8 Dynamic rheological analyses of NIPU samples. Influence of the average amine functionality on the storage modulus. *NIPU-fn=2.0* (●), *2.05* (■), *2.1* (×), *2.15* (◆), and *2.2* (▲).

The tangent delta (tan δ) is also a relevant factor to evaluate the flow of the polymers. If this factor is lower than 1, no flow appears. Fig. 9 confirms the previous interpretations. For the *NIPU-fn=2.0*, *2.05* and *2.1* samples, this factor quickly increases from the room temperature to become higher than 1. These evolutions highlight the flow and the low structuration of these samples. For the other samples with higher average amine functionalities, the loss factors remain constant on a wider domain and mainly lower than 1. Furthermore, the presence of a rubbery plateau for each NIPU sample reveals an elastomeric behaviour for these materials.

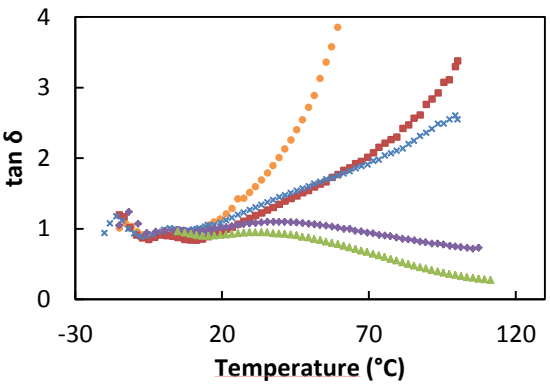

Fig. 9 Dynamic rheological analyses of NIPU samples. Influence of the average amine functionality on the tangent delta. *NIPU-fn=2.0* (●), *2.05* (■), *2.1* (×), *2.15* (◆), and *2.2* (▲).

Particular cases: Crosslinked materials

Considering the specific behaviour of the samples with a high average amine functionality (2.15 and 2.2), additional experiments were carried out for these materials in order to obtain further information on their morphologies and properties.

Dynamic mechanical analyses were performed on samples to complete the dynamic rheological analyses at low temperatures. Furthermore, it is also possible to evaluate the storage and the loss moduli, represented on Fig. 10. For both samples, a glassy plateau is observed from -80 to -40 °C

followed by a broad transition. The alpha relaxation temperature (T_α) can be estimated at the maximum of the loss modulus curve (Table 4). The samples reach then a rubbery state, due to the presence of crosslinking.

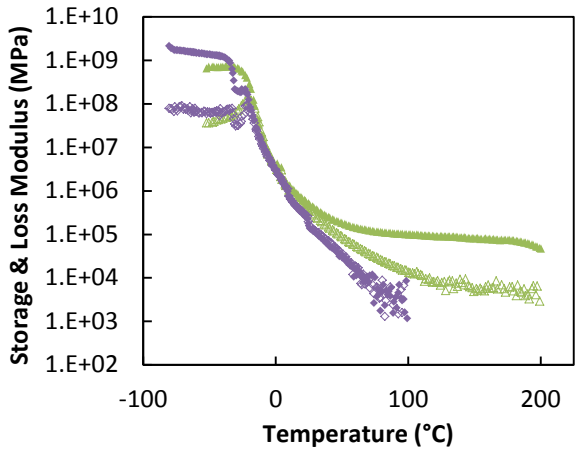

Fig. 10 DMTA curves of *NIPU-fn=2.2*: E' (▲) - E'' (△) and *2.15*: E' (◆) - E'' (◇).

The crosslink density, the degree of swelling and the gel content were determined for each crosslinked system *i.e.* for *NIPU-fn=2.15* and *2.2* samples.

The crosslink density (ν_e) can be obtained from Equation (1) which is derived from the rubber elasticity theory[46] where, R is the gas constant (8.31 J.mol-1.K^{-1}) and T is the temperature in Kelvin.

$$\nu_e = \frac{E}{3\,R\,T} \quad (1)$$

Since the elastic modulus (E) can be associated to the storage modulus (E') at temperatures well above T_g, E can be substituted by E' in Equation 1 to determine ν_e (in the rubbery region at T_α + 40 °C). Thus, the plateau of the elastic modulus in the rubbery state obtained from DMTA curves can be used to evaluate the crosslink density of NIPU materials.

Table 4 summarizes values of the crosslink density determined from Equation (1). As expected, the crosslink density increases with the amine functionality. It is thus possible to modulate NIPU properties. The higher crosslink density is obtained with an average amine functionality of 2.2. However, the values are quite low compared to conventional systems.[47, 48]

Table 4 Main characteristic values for crosslinked NIPU.

Samples	T_α a/ (°C)	T_α + 40 (°C)	E' b/ at T_α + 40 (Pa)	ν_e c/ (mol.m^{-3})	G d/ (%)	Q e/ (%)
NIPU-fn=2.15	-26	14	5.67 10^5	79	21	1.4
NIPU-fn=2.2	-20	20	6.58 10^5	90	70	1.6

a/ Alpha relaxation temperature determined from DMTA. b/ Storage modulus. c/ Crosslink density. d/ Gel content. e/ Degree of swelling.

The equilibrium degree of swelling (Q) was calculated from the swelling of NIPU in chloroform, using Equation (2). Where, W_P is the weight of dry polymer, W_S the weight of the solvent at equilibrium, d_P the density of the polymer and d_S the density of the solvent.

$$Q = \frac{W_P/d_P + W_S/d_S}{W_P/d_P} \quad (2)$$

The percentage of gel content (G) was determined from Equation (3). Where, W_{P0} is the initial sample weight.

$$G = \frac{W_P}{W_{P0}} * 100 \quad (3)$$

All these results confirm that the NIPU synthesized with the diamine of an average functionality of 2.2 is the highest crosslinked system with the highest gel content (Table 4). Compared with conventional PU, which are fully crosslinked at a functionality of 2.2, *NIPU-fn=2.2* contains 30 % of soluble fraction. This result is due to the secondary reactions.

Finally, uniaxial tensile tests were performed on the highest crosslinked NIPU, *NIPU-fn=2.2* in order to estimate its mechanical performances. Young's modulus E = 0.4 ± 0.1 MPa, tensile strength at break σ_{max} = 0.6 ± 0.2 MPa and elongation at break ε_{max} = 630 ± 80 % were determined from the corresponding stress-strain curve. In the literature, PU based on polyisocyanate with dimer fatty acids have similar elasticity and higher modulus.[43] However, NIPU with a crosslink network often present a very low elasticity, far from an elastomeric behaviour._ENREF_5 With an elongation at break higher than 600 %, NIPU synthesized from DDA1 and SB BisCC reveals to be a promising soft material with high elastomeric properties.

Conclusions

A solvent-free and catalyst-free method for preparing polyurethanes (PU) without harmful isocyanate was developed. All NIPU synthesized present biobased contents around 80 % (based on ^{14}C). Sebacic biscyclocarbonate and biobased dimer diamines (DDA) were used as building blocks for the synthesis of new biobased nonisocyanate polyurethane (NIPU). The resulting properties and behaviours were investigated.

All obtained NIPU are amorphous and show a low T_g suitable for various applications. Several average amine functionalities of DDA were used to determine the structure-properties relationships of the NIPU. Thermal and rheological analyses revealed that the modulation of the properties is possible through the control of the average amine functionalities of DDA. It was observed that the NIPU behaviour is linked to the crosslink degree, which can be adjusted. NIPU with the highest crosslinking displays high elasticity. This corresponding NIPU with original macromolecular architecture is a promising elastomer with a great potential to replace some conventional soft PU in the future.

These results clearly show the possibility to use such biobased architectures to design novel environmental and health friendly PU with high performances in different areas in which biobased and durable systems are required (*e.g.* automotive, building …). Furthermore, with their chemical structures, molar masses … one can imagine a wide range of applications in the field of adhesives. To fulfil some specific requirements, these biobased polymers could also be formulated to elaborate multiphase systems.

Acknowledgements

The authors thank the Alsace Region, the urban community of Strasbourg, SOPREMA and PSA Peugeot Citroën for their financial supports. Croda and Huntsman are also acknowledged for having kindly provided dimer diamines and glycerol

carbonate, respectively. The authors would like to acknowledge Prof. Jean-Pierre Pascault (IMP-INSA Lyon, France) and Dr. Sébastien Gallet (ICPEES Strasbourg, France) for helpful discussions.

Notes and references

[a] BioTeam/ICPEES-ECPM, UMR 7515, Université de Strasbourg, 25 rue Becquerel, 67087 Strasbourg Cedex 2, France.
* Corresponding author: Prof. Luc Avérous, Phone: +33 3 68 85 27 84, Fax: +33 3 68 85 27 16, E-mail: luc.averous@unistra.fr.
† Electronic Supplementary Information (ESI) available: Characterization of sebacic biscyclocarbonate (SB BisCC) and nonisocyanate polyurethane (*NIPU-fn=2.0*). See DOI: 10.1039/ x0xx00000x

1. O. Bayer, *Angew. Chem.*, 1947, **59**, 257-272.
2. X. Baur, W. Marek, J. Ammon, A. B. Czuppon, B. Marczynski, M. Raulf-Heimsoth, H. Roemmelt and G. Fruhmann, *Int. Arch. Occup. Environ. Health*, 1994, **66**, 141-152.
3. Commission Regulation (EC) No. 552/2009 amending Regulation (EC) No. 1907/2006 of the European Parliament and of the Council on the Registration, Evaluation, Authorisation and Restriction of Chemicals (REACH) as regards Annex XVII, in *Official Journal*, 2009, vol. L 164, pp. 7-31.
4. NIOSH, U.S. Department of Health and Human Services, Centers for Disease Control and Prevention, Publication No. 2004-116, Cincinnati, 2004.
5. J. Guan, Y. H. Song, Y. Lin, X. Z. Yin, M. Zuo, Y. H. Zhao, X. L. Tao and Q. Zheng, *Ind. Eng. Chem. Res.*, 2011, **50**, 6517-6527.
6. M. S. Kathalewar, P. B. Joshi, A. S. Sabnis and V. C. Malshe, *RSC Adv.*, 2013, **3**, 4110-4129.
7. B. Nohra, L. Candy, J.-F. Blanco, C. Guerin, Y. Raoul and Z. Mouloungui, *Macromolecules (Washington, DC, U. S.)*, 2013, **46**, 3771-3792.
8. P. Deepa and M. Jayakannan, *J. Polym. Sci., Part A: Polym. Chem.*, 2008, **46**, 2445-2458.
9. D. V. Palaskar, A. Boyer, E. Cloutet, C. Alfos and H. Cramail, *Biomacromol.*, 2010, **11**, 1202-1211.
10. P. Deepa and M. Jayakannan, *J. Polym. Sci., Part A: Polym. Chem.*, 2007, **45**, 2351-2366.
11. *US Pat.*, 2,802,022, American Cyanamid Company, 1957.
12. *US Pat.*, 3,072,613, Union Carbide Corporation, 1963.
13. N. Kihara and T. Endo, *J. Polym. Sci., Part A: Polym. Chem.*, 1993, **31**, 2765-2773.
14. A. Steblyanko, W. M. Choi, F. Sanda and T. Endo, *J. Polym. Sci., Part A: Polym. Chem.*, 2000, **38**, 2375-2380.
15. H. Tomita, F. Sanda and T. Endo, *J. Polym. Sci., Part A: Polym. Chem.*, 2001, **39**, 851-859.
16. B. Ochiai, S. Inoue and T. Endo, *J. Polym. Sci., Part A: Polym. Chem.*, 2005, **43**, 6282-6286.
17. D. L. Tang, D. J. Mulder, B. A. J. Noordover and C. E. Koning, *Macromol. Rapid Commun.*, 2011, **32**, 1379-1385.
18. I. Javni, D. P. Hong and Z. S. Petrovic, *J. Appl. Polym. Sci.*, 2008, **108**, 3867-3875.
19. M. Bahr and R. Mulhaupt, *Green Chem.*, 2012, **14**, 483-489.
20. M. Bahr, A. Bitto and R. Mulhaupt, *Green Chem.*, 2012, **14**, 1447-1454.
21. O. L. Figovsky and L. D. Shapovalov, *Macromol. Symp.*, 2002, **187**, 325-332.
22. O. L. Figovsky and L. D. Shapovalov, Manchester, 2005.
23. *US Pat.*, 7,820,779, Polymate, Ltd. Nanotech Industries, Inc., 2009.
24. S. Benyahya, M. Desroches, R. Auvergne, S. Carlotti, S. Caillol and B. Boutevin, *Polym. Chem.*, 2011, **2**, 2661-2667.
25. M. O. Sonnati, S. Amigoni, E. P. Taffin de Givenchy, T. Darmanin, O. Choulet and F. Guittard, *Green Chem.*, 2013, **15**, 283-306.
26. F. C. Naughton, *J. Am. Oil Chem. Soc.*, 1974, **51**, 65-71.
27. C. D. Diakoumakos and D. L. Kotzev, *Macromol. Symp.*, 2004, **216**, 37-46.
28. H. Tomita, F. Sanda and T. Endo, *J. Polym. Sci., Part A: Polym. Chem.*, 2001, **39**, 3678-3685.
29. H. Tomita, F. Sanda and T. Endo, *J. Polym. Sci., Part A: Polym. Chem.*, 2001, **39**, 860-867.
30. F. Camara, S. Benyahya, V. Besse, G. Boutevin, R. Auvergne, B. Boutevin and S. Caillol, *Eur. Polym. J.*, 2014, **55**, 17-26.
31. E. Hablot, B. Donnio, M. Bouquey and L. Averous, *Polymer*, 2010, **51**, 5895-5902.
32. C. Bueno-Ferrer, E. Hablot, F. Perrin-Sarazin, M. C. Garrigós, A. Jiménez and L. Averous, *Macromol. Mater. Eng.*, 2012, **297**, 777-784.
33. I. Javni, D. P. Hong and Z. S. Petrović, *J. Appl. Polym. Sci.*, 2013, **128**, 566-571.
34. A. S. More, T. Lebarbé, L. Maisonneuve, B. Gadenne, C. Alfos and H. Cramail, *Eur. Polym. J.*, 2013, **49**, 823-833.
35. A. Saralegi, L. Rueda, B. Fernández-d'Arlas, I. Mondragon, A. Eceiza and M. A. Corcuera, *Polym. Int.*, 2013, **62**, 106-115.
36. A. Boyer, E. Cloutet, T. Tassaing, B. Gadenne, C. Alfos and H. Cramail, *Green Chem.*, 2010, **12**, 2205-2213.
37. E. Delebecq, J.-P. Pascault, B. Boutevin and F. Ganachaud, *Chem. Rev. (Washington, DC, U. S.)*, 2013, **113**, 80-118.
38. J. H. Saunders, *Rubber Chem. Technol.*, 1959, **32**, 337-345.
39. I. Javni, Z. S. Petrović, A. Guo and R. Fuller, *J. Appl. Polym. Sci.*, 2000, **77**, 1723-1734.

40. B. Ochiai and T. Utsuno, *J. Polym. Sci., Part A: Polym. Chem.*, 2013, **51**, 525-533.

41. V. Besse, R. Auvergne, S. Carlotti, G. Boutevin, B. Otazaghine, S. Caillol, J.-P. Pascault and B. Boutevin, *React. Funct. Polym.*, 2013, **73**, 588-594.

42. X. Liu, K. Xu, H. Liu, H. Cai, Z. Fu, Y. Guo and M. Chen, *Macromol. Res.*, 2012, **20**, 642-649.

43. C. Bueno-Ferrer, E. Hablot, M. Del Carmen Garrigos, S. Bocchini, L. Averous and A. Jiménez, *Polym. Degrad. Stab.*, 2012, **97**, 1964-1969.

44. S. Yadav, F. Zafar, A. Hasnat and S. Ahmad, *Prog. Org. Coat.*, 2009, **64**, 27-32.

45. J. P. Pascault and R. J. J. Williams, in *Thermosets: Structure, Properties And Applications*, ed. Q. Guo, Woodhead Publishing Ltd., 2012, pp. 3-27.

46. I. M. Ward and J. Sweeney, in *Mechanical Properties of Solid Polymers*, John Wiley & Sons Ltd., 2012, pp. 61-85.

47. A. Gerbase, C. Petzhold and A. Costa, *J. Am. Oil Chem. Soc.*, 2002, **79**, 797-802.

48. Q. Ma, X. Liu, R. Zhang, J. Zhu and Y. Jiang, *Green Chem.*, 2013, **15**, 1300-1310.

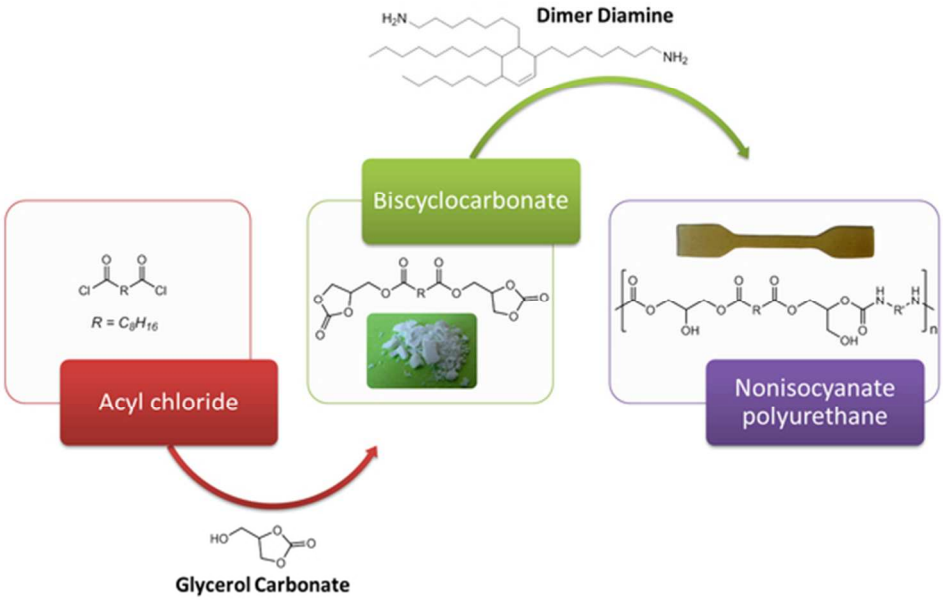

Graphical Abstract (600*600)
54x35mm (300 x 300 DPI)